Chemical Vapor Deposition of Zinc from Diallyl Zinc Precursors

Jinwoo Cheon,[†] Lawrence H. Dubois,*[,‡] and Gregory S. Girolami*[,†]

School of Chemical Sciences and Materials Research Laboratory, University of Illinois at Urbana–Champaign, 505 South Mathews Avenue, Urbana, Illinois 61801, and AT&T Bell Laboratories, 600 Mountain Avenue, Murray Hill, New Jersey 07974

Received February 24, 1994. Revised Manuscript Received August 23, 1994[⊗]

The organometallic compounds bis(allyl)zinc and bis(2-methylallyl)zinc have been shown to serve as MOCVD precursors for the deposition of zinc at temperatures as low as 150 °C. The deposits on Si(100) wafers, quartz, copper, and aluminum consist of aggregates of hexagonal plates and columns. On silicon(100) substrates and at low background pressures (10^{-4} Torr), the zinc crystals are oriented preferentially with their *c* axes perpendicular to the silicon surface. The organic byproducts generated under CVD conditions are 1,5-hexadiene (76 mol %), 2-methyl-1,4-pentadiene (14 mol %), and propene (10 mol %); except for the pentadiene product, analogous hydrocarbons in similar amounts are formed when bis(2-methylallyl)zinc is used as the precursor. In situ spectroscopic studies on single-crystal Cu(111) substrates show that bis(allyl)zinc transfers its allyl groups to the surface below 250 °C; the surface-bound allyl groups are probably bound in a trihapto fashion. On clean surfaces, the allyl groups react between 10 and 130 °C to give propene and smaller amounts of 2-methyl-1,4-pentadiene. The propene is the result of transfer of a hydrogen atom to the surface allyl groups; the source of the hydrogen atoms has been traced to the sacrificial fragmentation of some of the allyl groups. The dehydrogenation of some of the surface allyl groups also gives rise to hydrogen-deficient hydrocarbon fragments, which eventually convert to a carbonaceous overlayer. Once the overlayer is formed, fragmentation of allyl groups is inhibited and, instead, coupling of allyl groups to 1,5-hexadiene is the predominant reaction channel. Passage of a mixture of bis(2-methylallyl)zinc and bis(2-methylallyl)palladium over substrates at 250 °C and 10^{-2} Torr results in the deposition of Zn/Pd alloys.

Introduction

Dialkylzinc compounds are the most commonly used precursors for the metal–organic chemical vapor deposition (MOCVD) of zinc-containing materials such as the II–VI compound semiconductors used in the manufacture of light emitting diodes and solar cells.[1–4] Typically, thin films of zinc-containing binary semiconductors such as ZnO,[5,6] ZnS,[7] ZnSe,[8] and ZnTe[9] and ternary semiconductors[9,10] such as $ZnS_{1-x}Se_x$ and $Zn_{1-x}Cd_xS$ are deposited from dimethyl- or diethylzinc in combination with H_2O, O_2, H_2S, H_2Se, or gaseous Te_2. In addition, zinc alkyls have been used to introduce zinc as a p-type dopant into III–V semiconductors.[3] Because impurities can degrade the electrical properties of compound semiconductors even at the 500 ppb level,[1–3] alkylzinc precursors cannot be used in some instances due to the incorporation of excessive amounts of carbon into the growing film. Occasionally, the addition of dihydrogen as a carrier gas is effective in decreasing carbon contaminants to an acceptable level.

Diethylzinc is also useful for the deposition of crystalline zinc films by means of plasma-assisted CVD.[11] In addition, zinc films have been grown on various substrates such as quartz, GaAs, and InP from dimethylzinc and diethylzinc by photochemical/laser assisted vapor depositions.[12–15] While carbon contaminants were present when dimethylzinc was used as a precursor,[12] highly pure zinc films were obtained by photolysis of diethylzinc at 248 nm with an ArF^+ or dye laser.[16] Zinc films can also be prepared by direct evaporation.[17]

The thermolyses of dimethylzinc and diethylzinc have been studied in order to elucidate their decomposition chemistry.[18] Dimethylzinc decomposes in the vapor

[†] The University of Illinois.
[‡] AT&T Bell Laboratories. Current address: Advanced Research Projects Agency, Arlington, VA.
[⊗] Abstract published in *Advance ACS Abstracts,* October 1, 1994.

(1) Dupuis, R. D. *Science* **1984**, *226*, 623–629.
(2) Moss, R. H. *Chem. Brit.* **1983**, 733–737.
(3) Williams, J. O. *Angew. Chem., Int. Ed. Engl.* **1989**, *28*, 1110–1120.
(4) Morosanu, C. E. *Thin Films by Chemical Vapor Deposition*; Elsevier: New York, 1990; Chapter 12.
(5) Roth, A. P.; Williams, D. F. *J. Electrochem. Soc.* **1981**, *128*, 2684–2686.
(6) Cockyne, B.; Wright, P. J. *J. Cryst. Growth* **1984**, *68*, 223–230.
(7) Strong R. L.; Smith, P. B. *J. Vac. Sci. Technol. A* **1990**, *8*, 1544–1548.
(8) Yeh, M. Y.; Hu, C. C.; Lin, G. L.; Lee, M. K. *Thin Solid Films* **1992**, *215*, 142–146.
(9) Chu, T. L.; Chu, S. S.; Firzst, F.; Herrington, C. *J. Appl. Phys.* **1986**, *59*, 1259–1263.
(10) Fujita, S.; Matsuda, Y.; Sasaki, S. *J. Cryst. Growth* **1984**, *68*, 231–236.
(11) James, W. J.; Tseng, P.-L. *J. Vac. Sci. Technol. A* **1985**, *3*, 2634–2638.
(12) Johnson, W. E.; Schlie, L. A. *Appl. Phys. Lett.* **1982**, *40*, 798–801.
(13) Eden, J. G. *Photochemical Vapor Deposition*; Wiley: New York, 1992; Chapter 4.
(14) Saitoh, T.; Shimada, T.; Migitaka, M.; Tarui, Y. *J. Non-Cryst. Solids* **1983**, *59*, 715–718.
(15) Ehrlich, D. J.; Osgood, Jr. R. M.; Deutsch, T. F. *J. Vac. Sci. Technol.* **1982**, *21*, 23–32.
(16) Larciprete, R.; Borsella, E. *Nuovo Cim.* **1989**, *11D*, 1603–1613.
(17) Heulin, B.; Sealy, J. *Thin Solid Films* **1983**, *105*, 227–235.
(18) Kuniya, Y.; Deguchi, Y.; Ichida, M. *Appl. Organomet. Chem.* **1991**, *5*, 337–347.

0897-4756/94/2806-2279$04.50/0

phase at 270–370 °C to deposit metallic zinc that contains "graphitic" carbon in the form of highly polymerized hydrogen-deficient hydrocarbons. Methane was the principal gas phase byproduct, although small amounts of ethane, ethylene, propane, and propene were also detected. In comparison, diethylzinc decomposes at 175–225 °C to deposit metallic zinc that contains less graphitic carbon; ethane and *n*-butane were the principal gas-phase products. In fact, diethylzinc has been used more frequently as a zinc source than dimethylzinc, despite its lower vapor pressure, because it tends to give purer films.[5,7,11]

Thermal decomposition studies of dimethylzinc and diethylzinc on a Si(100)-2×1 surface under UHV conditions have also been reported.[19] Upon heating a dosed Si surface, the alkyl groups transfer to silicon and zinc metal desorbs; at higher temperatures, the silicon-bound alkyl groups decompose to yield hydrogen, various hydrocarbons, and residual surface carbon.

We have previously demonstrated that allyl derivatives of the transition elements are often effective MOCVD precursors.[20,21] Other workers have also used binary allyl complexes to deposit films of transition metals and certain metal carbide phases; mixed-ligand complexes containing allyl ligands have also been used as CVD sources for metal films.[22–28] The utility of allyl complexes is in part a consequence of their ability to react with hydrogen to form propene and to reductively eliminate hexadiene at relatively low temperatures; both of these processes free the metal atom from its ligands and promote the growth of a clean metallic film.

We now describe the use of the zinc allyl compounds[29] bis(allyl)zinc and bis(2-methylallyl)zinc to deposit high-purity zinc. Mechanistic studies of the deposition process are also detailed.

Results and Discussion

Metal–Organic Chemical Vapor Deposition of Zinc. Deposition of zinc from the bis(allyl)zinc, **1**, has been carried out at three temperatures (150, 250, and 290 °C) and at two system background pressures (10^{-2} and 10^{-4} Torr). Depositions conducted at the latter two temperatures give virtually identical results: passage of **1** over a variety of substrates, including Si(100) wafers, quartz, copper, and aluminum, yields bright silvery deposits. Deposits up to 20 μm thick can be grown over several hours; the deposition rate on silicon is ca. 7 μm/h at 290 °C and 10^{-2} Torr. X-ray photoelectron spectra (XPS) and Auger electron spectra (AES) indicate that the deposits are essentially pure zinc metal (Figures 1 and 2). Depth profiles calculated from Auger signal intensities show that some oxygen and carbon are present at the surface of the deposits, but that these species are not detectable in the interior (<1 atomic %). Depositions conducted with H_2 as a carrier gas showed that the presence of H_2 had no significant effect on the purity (or morphology) of the deposits.

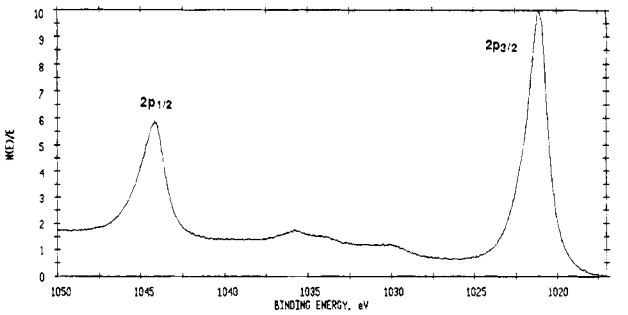

Figure 1. X-ray photoelectron spectrum in the Zn 2p region of a zinc film deposited from $Zn(C_3H_5)_2$ on Si(100) at 290 °C and 10^{-2} Torr.

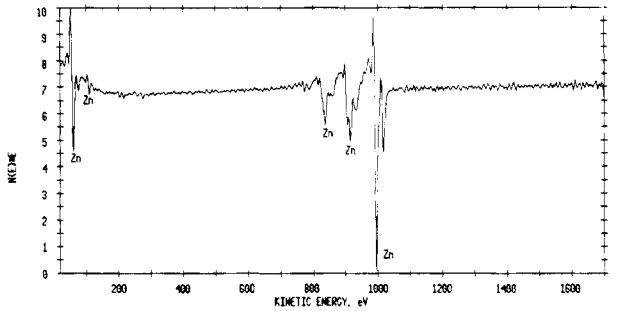

Figure 2. Auger survey spectrum of a zinc film deposited from $Zn(C_3H_5)_2$ on Si(100) at 290 °C and 10^{-2} Torr.

In contrast to the above results, passage of **1** over substrates at temperatures below 150 °C yields very thin deposits (ca. 0.1 μm); the XRD patterns of these deposits contain diffraction peaks due to zinc, but the XPS and Auger spectra again show that there is an oxide overlayer that presumably is formed by air oxidation after the deposits are removed from the deposition chamber. Owing to the thinness of the deposits, the composition of the underlying bulk phase cannot be determined by sputtering away the oxide overlayer because the sputtering quickly removes all of the zinc-containing material and exposes the underlying substrate.

Scanning electron micrographs of the deposits grown on Si(100) at 290 °C and ca. 10^{-2} Torr consisted of granules with hexagonal faces (Figure 3). Deposits grown at ca. 10^{-4} Torr consisted of hexagonal plates and columns, which exhibit strong (002) and (004) X-ray diffraction peaks (Figure 4a). This result suggests that the crystals grown under the latter conditions are preferentially oriented with their *c* axes perpendicular to the substrate. These deposits are not truly pseudomorphic, however, as shown by the presence of weak (100) and (101) peaks in the diffraction profile and by the nonuniform orientations of the crystals as seen in the electron micrographs. In contrast, the deposits grown at ca. 10^{-2} Torr exhibit a diffraction pattern

(19) Rueter, M. A.; Vohs, J. M. *Mater. Res. Soc. Symp. Proc.* **1991**, *204*, 403–408.
(20) Gozum, J. E.; Jensen, J. A.; Pollina, D. M.; Girolami, G. S. *J. Am. Chem. Soc.* **1988**, *110*, 2688–2689.
(21) Gozum, J. E. Ph.D. Thesis, University of Illinois at Urbana–Champaign, March 1991.
(22) Feurer, E.; Suhr H. *Thin Solid Films* **1988**, *157*, 81–86.
(23) Kaesz, H. D.; Williams, R. S.; Hicks, R. F., Chen, Y.-J.; Xue, Z.; Xu, D.; Shuh, D. K.; Thridandam, H. *Mater. Res. Soc., Symp. Proc.* **1989**, *131*, 395–400.
(24) Kaesz, H. D.; Williams, R. S.; Hicks, R. F.; Zink, J. I.; Chen, Y.-J.; Muller, H. J.; Xue, Z.; Xu, D.; Shuh, D. K.; Kim, Y. K. *New J. Chem.* **1990**, *14*, 527–534.
(25) Smith, D. C.; Patillo, S. G.; Elliot, N. E.; Zocco, T. G.; Burns, C. J.; Laia, J. R.; Sattelberger, A. P. *Mater. Res. Soc. Sym. Proc.* **1990**, *168*, 369–374.
(26) Dryden, N. H.; Kumar, R.; Ou, E.; Rashidi, M.; Roy, S.; Norton, P. R.; Puddephatt, R. J. *Chem. Mater.* **1991**, *3*, 677–685.
(27) Kirss, R. U.; Chen, J.; Hallock, R. B. *Mater. Res. Soc., Symp. Proc.* **1992**, *250*, 303.
(28) Kirss, R. U. *Appl. Organomet. Chem.* **1992**, 6, 609–617.
(29) Thiele, K. H.; Zdunneck, P. *J. Organomet. Chem.* **1965**, *4*, 10–17.

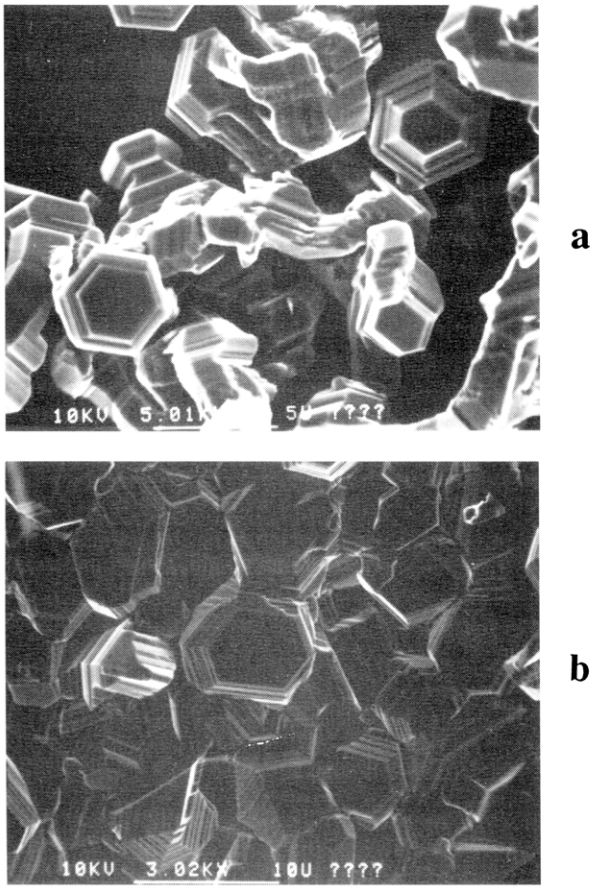

Figure 3. Scanning electron micrographs of zinc films deposited from $Zn(C_3H_5)_2$ on Si(100) (a) at 290 ° C and 10^{-4} Torr and (b) at 290 °C and 10^{-2} Torr.

consistent with a random distribution of crystal orientations (Figure 4b).

The pressure dependence of the distribution of crystal orientations reflects a subtle difference in the nucleation and growth processes that is probably related to the high vapor pressure or low melting point of zinc metal. One possibility is that at a background pressure of 10^{-4} Torr, the zinc atoms are mobile and able to find the most preferred sites; as a result, nucleation and subsequent crystal growth occurs in an oriented fashion.[30] At a system background pressure of 10^{-2} Torr (i.e., at lower pumping speeds), water, oxygen, or hydrocarbons in the hot zone could lead to the formation of a thin oxide or carbonaceous overlayer that inhibits the mobility of the zinc atoms, so that oriented growth does not occur. As we showed above, both oxygen and carbon are in fact present at the surface of the deposits.

The measured resistivity of a Zn film grown at 250 °C and 10^{-2} Torr on a silicon wafer is 20 ± 5 $\mu\Omega$ cm at room temperature, which is significantly higher than that of polycrystalline bulk zinc (5.9 $\mu\Omega$ cm).[31] This result is not surprising in view of the morphology of the deposit as shown by the electron micrographs.

Zinc films can also be grown on both Si(100) wafers and copper foils from bis(2-methylallyl)zinc, **2**, at 150–290 °C and 10^{-2} Torr. AES shows that the interiors of the deposits are free of carbon and oxygen contaminants, and X-ray diffraction (XRD) analyses show that the deposits are polycrystalline. Scanning electron micrographs show that deposits on a silicon wafer consist of granules with hexagonal faces, having almost the same features as deposits grown from the allyl precursor **1**. We thus conclude that there are no significant differences in the morphology or quality of the deposits obtained from **1** and **2**.

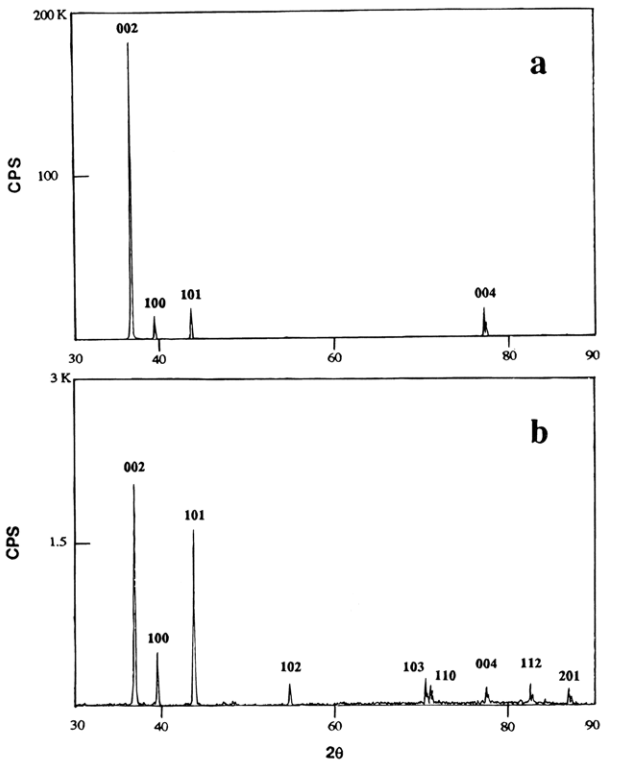

Figure 4. X-ray powder diffraction profile of a zinc film deposited from $Zn(C_3H_5)_2$ on Si(100) (a) at 290 °C and 10^{-4} Torr and (b) at 290 °C and 10^{-2} Torr.

Static Vacuum Depositions and Analyses of the Gaseous Byproducts. Preliminary analyses of the gaseous byproducts generated during the deposition of zinc from the allyl precursor **1** have been carried out in situ under dynamic vacuum conditions using a quadrupole mass spectrometer attached to our CVD apparatus. The mass spectra indicate that propene and hexadiene(s) are the principal organic byproducts. The hexadiene isomer (or isomers) formed can not be determined unambiguously from the mass spectrum because the various hexadiene isomers have very similar fragmentation patterns. We have, however, repeated the CVD experiments in a closed static vacuum system in order to collect, identify, and quantify the gaseous byproducts generated when zinc is deposited from these organozinc precursors.

Under a static vacuum (10^{-2} Torr), **1** was sublimed into a deposition zone maintained at 290 °C, and the gaseous products were collected in a liquid N_2 cooled NMR tube. After deposition was complete, the NMR tube was flame sealed and the the products were analyzed by NMR and GC/MS methods. Quantitative NMR analyses reveal that the major product is 1,5-hexadiene (76 mol %) and the minor products are 2-methyl-1,4-pentadiene (14 mol %) and propene (10 mol %). The absolute yields of these products show that 0.71 equiv of 1,5-hexadiene, 0.13 equiv of 2-methyl-1,4-

(30) Ohring, M. *The Materials Science of Thin Films*; Academic: Boston, 1992; Chapters 3, 5, and 10. For reference, the melting point of zinc is 420 °C.

(31) *Handbook of Chemistry and Physics*, 68th ed.; Weast, R. C., Ed.; CRC Press: Cleveland, OH, 1987; p F-122.

pentadiene, and 0.10 equiv of propene are formed per mol of $Zn(allyl)_2$ consumed. These organic byproducts account for 89% of the carbon and 90% of the hydrogen originally present in the precursor. Some of the carbon and hydrogen that is unaccounted for probably was lost because collection of the volatile byproducts cannot be effected with 100% efficiency; traces of carbon are also present at the surface of the zinc deposits. The interior of the reflective white deposit grown in this experiment is essentially pure zinc (>98%) as shown by elemental analysis.

Similarly, static vacuum CVD depositions were conducted from the 2-methylallyl precursor **2** at 290 °C and 10^{-2} Torr. Quantitative ^1H NMR analyses show that 0.82 equiv of 2,5-dimethyl-1,5-hexadiene, 0.07 equiv of 2,5-dimethyl-2,4-hexadiene, and 0.07 equiv of isobutylene are formed per mole of **2** consumed; 92% of the carbon and 93% of the hydrogen originally present in the precursor can thus be accounted for. The product distribution is very similar to that generated from **1**, except that no substituted pentadienes are formed from **2**; instead, small amounts of a conjugated hexadiene are seen.

Hydrogen Balance. Owing to the presence of propene, the hydrogen-to-carbon ratio among the gaseous CVD byproducts is *larger* than the ratio in the organozinc precursor **1**. A similar situation pertains for depositions conducted from the 2-methylallyl precursor **2**, where isobutylene is one of the gaseous byproducts. It is therefore of interest to determine where the extra hydrogen comes from. There are at least two possible sources: adventitious water and hydrogen atoms from other allyl groups.

Small amounts of gaseous water are always present during deposition; in addition, there are hydroxyl groups present on the substrates and the walls of the chamber that could serve as proton sources. Hydrolysis of some of the allyl groups would necessarily be accompanied by the formation of an oxide overlayer on the films. Such a sacrificial fragmentation reaction would generate surface hydrogen atoms, which could transfer to intact allyl groups and generate propene. Sacrificial fragmentation of some of the allyl groups would necessarily be accompanied by the formation of a hydrogen-deficient carbon overlayer on the films. Recall that both oxygen and carbon are present on the surfaces of the zinc deposits as shown by the AES spectra before sputtering.

Interestingly, the relative amounts of propene and hexadiene formed change during the course of zinc deposition as judged by mass spectrometry (Figure 5). At the beginning of a run, propene peaks dominate the mass spectrum while the hexadiene peaks are small. As the deposition progresses, the hexadiene peaks become much more intense and very little propene is observed. These observations suggest that the hydrogen source responsible for the formation of propene is depleted with time. This result can be easily understood if water or surface hydroxyl groups serve as the source of hydrogen atoms, since this finite source would eventually be consumed. Note that the sacrificial fragmentation of allyl groups could also slow down with time if the accumulated hydrogen-deficient carbon overlayer worksas a protective coating and prohibits further fragmentation of allyl groups.[32]

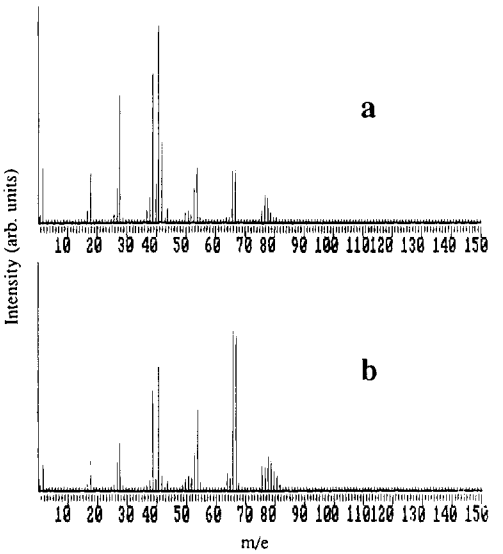

Figure 5. Mass spectra of the products exiting the hot zone during CVD of Zn from $Zn(C_3H_5)_2$ at 290 °C and 10^{-4} Torr. (a) Spectrum obtained 5 min after the beginning of the run. Propene (m/e = 42) is dominant and only small amounts of 1,5-hexadiene (m/e = 67) are seen. (b) Spectrum obtained 15 min after the beginning of the run. 1,5-Hexadiene is now dominant. The peaks near m/e 78 are due to background impurities in the mass spectrometer.

Finally, we note that propene is also generated as a minor product (along with hexadiene) during the deposition of palladium films from the allylpalladium precursor $Pd(allyl)_2$[20,21] and during the pyrolysis of the allylselenium and -tellurium compounds $Se(allyl)_2$ and $Te(allyl)_2$.[33] A concerted "ene" mechanism involving transfer of an α-hydrogen atom from one allyl group to another has been proposed to account for the formation of propene when $Se(allyl)_2$ is thermolyzed.[33] Interestingly, thermolyses of binary allyl derivatives of Hf, Cr, Mo, W, and Rh give propene almost exclusively (>94 mol %);[27,28] in these cases it has usually been assumed that the extra hydrogen atom necessary for the conversion of allyl groups to propene is abstracted from other allyl groups.

Ultrahigh-Vacuum Studies on Cu(111) Single Crystals. Although the static vacuum experiments afford indirect information about the reactions that take place during deposition of zinc, they do not provide any *direct* evidence of the intermediate species present and the dynamic processes they undergo. To obtain such information, studies of the behavior of $Zn(allyl)_2$ on a Cu(111) single-crystal surface have been carried out.

In an ultrahigh-vacuum chamber, a Cu(111) single crystal was dosed with submonolayer amounts (ca. 0.2 langmuir) of bis(allyl)zinc at −20 °C. The AES spectrum of the as-dosed surface clearly shows the presence zinc and carbon in the ratio expected for intact precursor molecules (found, 1:5; calcd, 1:6; Figure 6a). Temperature-programmed desorption (TPD) studies show that both propene (m/e = 42, 41) and 2-methyl-1,4-pentadiene (m/e = 67, 41) desorb between 10 and 130 °C (Figure 7). The integrated desorption mass spectrum

(32) Carbonaceous overlayers often decrease the propensity of metal surfaces to promote hydrocarbon fragmentation processes. See: Lin, W.; Nuzzo, R. G.; Girolami, G. S., manuscript in preparation.

(33) Kirss, R. U.; Brown, D. W.; Higa, K. T.; Gedridge, R. W. *Organometallics* **1991**, *10*, 3589−3596.

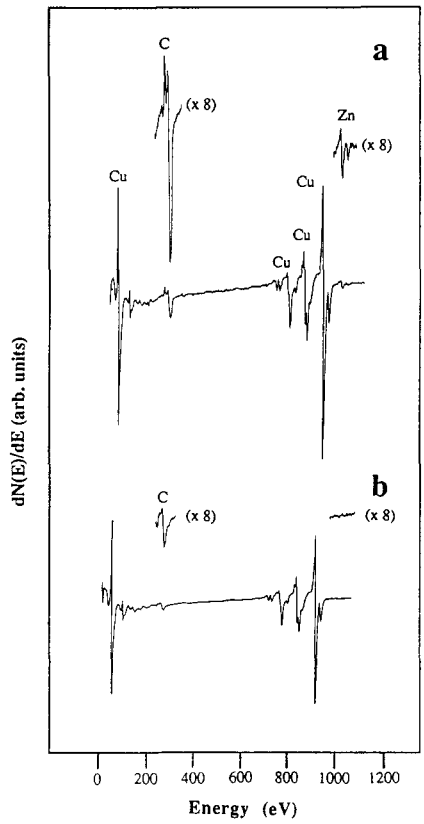

Figure 6. Auger survey spectra of $Zn(C_3H_5)_2$ dosed on Cu(111) at 250 K: (a) spectrum taken after dosing at 250 K and (b) spectrum of residual carbon generated after the surface had been heated to 900 K.

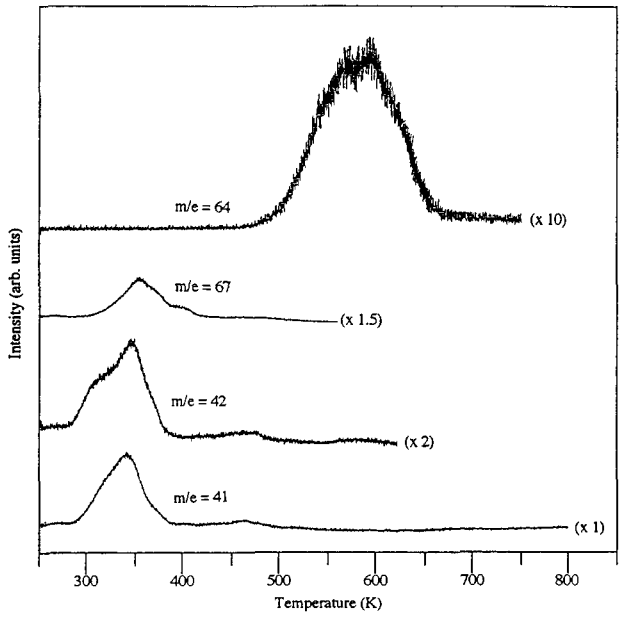

Figure 7. Temperature-programmed desorption traces for Zn(allyl)$_2$ dosed onto a Cu(111) single crystal at 250 K. The m/e = 42 channel tracks desorption of propene, m/e = 67 tracks desorption of dienes (1,5-hexadiene, 2-methyl-1,4-pentadiene), m/e = 41 tracks desorption of both propene and dienes, and m/e = 64 tracks desorption of atomic zinc.

(IDMS) taken between 30 and 130 °C indicates that propene is the major product and 2-methyl-1,4-pentadiene the minor product. Essentially no 1,5-hexadiene is generated, as shown by the absence of a peak at m/e = 54 in the IDMS spectrum (Figure 8). Between 230 and 380 °C, the desorption of atomic zinc (m/e = 64) is also observed (T_{max} = 310 °C).

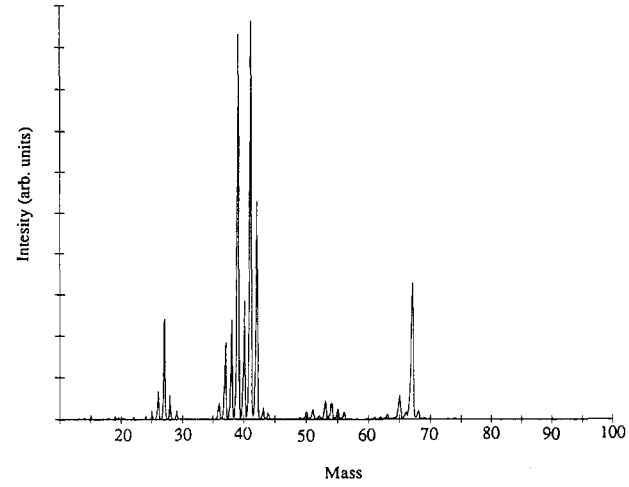

Figure 8. Integrated desorption mass spectrum of the products desorbing between 300 and 400 K from a Cu(111) surface dosed at 250 K with Zn(allyl)$_2$.

The presence of large amounts of propene in the desorption experiments clearly indicates that the "extra" hydrogen appearing in the gaseous byproducts under UHV conditions arises via sacrificial fragmentation of allyl ligands, since only vanishingly small amounts of water are present in the vacuum system. Consistent with this view, the Auger electron spectrum, taken after a TPD experiment in which the surface had been heated to 630 °C, shows that a carbonaceous overlayer remains on the surface (Figure 6b). Under CVD conditions, this carbonaceous overlayer evidently "percolates" to the surfaces of the deposits, since carbon was not observed to be present in the film interiors. Such "surfactant" behavior has been noted in other thin film growth processes.

In situ Infrared Studies on Cu(111) Single Crystals. To identify the structures of the surface species present on the substrates at different temperatures, we carried out reflection–absorption infrared (RAIR) studies of Cu(111) surfaces dosed at −70 °C with bis(allyl)zinc. The RAIR spectrum taken after dosing is consistent with the presence of a multilayer of intact bis(allyl)zinc molecules: the strong peak at 1536 cm^{-1} is assignable to a C–C stretching mode of such species,[34,35] and peaks due to C–H stretching modes (3064, 2991, 2950, and 2922 cm^{-1}) and C–H in-plane bending modes (1439, 1387, 1268, 1217, 1040, 999, and 957 cm^{-1}) are very similar to those present in the infrared spectrum of a bulk sample of **1**.

When the dosed surface is heated to −20 °C, the multilayer desorbs and the intensities of the C–H and C–C modes decrease nearly to zero (Figure 9). Surface-bound allyl groups must still be present in submonolayer amounts at this temperature, however, since the TPD experiments described above show that significant quantities of propene desorb upon heating the surface above 30 °C. The RAIR experiment is governed by the selection rule that only modes whose transition mo-

(34) Benn, R.; Grondey, H.; Lehmkuhl, H.; Nehl, H.; Angermund, K.; Kruger, C. *Angew. Chem., Int. Ed. Engl.* **1987**, *26*, 1279–1280.

(35) Nakamoto, K. *Infrared and Raman Spectra of Inorganic and Coordination Compounds*, Wiley: New York, 1986. The allyl C–H out-of-plane bending modes between 700 and 850 cm^{-1} are below the 900 cm^{-1} cutoff of the MCT detector.

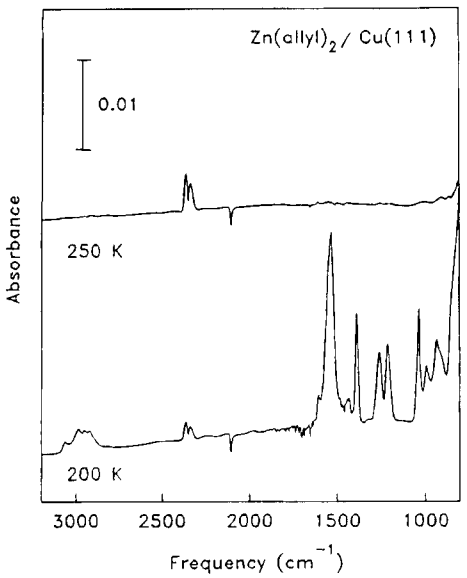

Figure 9. Temperature dependence of the RAIR spectra of $Zn(C_3H_5)_2$ dosed on Cu(111) at 200 K.

ments have nonzero projections onto the surface normal will be observable; vibrations whose transition directions are parallel with the surface will have zero intensity. The absence of features in the RAIR spectrum at −20 °C suggests that the allyl groups are oriented with their planes parallel with the surface (or nearly so): η^3-allyl group bound parallel to surface will show essentially no IR features between 4000 and 900 cm^{-1} because the C−H and C−C vibrational modes in this frequency range are all largely in-plane motions.[30] Since the allyl groups are σ-bound in both **1** and **2**, we conclude that at −20 °C they have transferred to the copper surface:

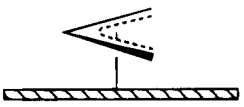

Above 30 °C, the surface-bound allyl groups fragment as shown by the TPD studies, but no further changes in the RAIR spectra are seen.

Mechanism of Zinc Deposition. Several different mechanisms could account for the predominance of 1,5-hexadiene among the organic byproducts generated during the deposition of zinc from **1** and **2**, and these can be classified broadly as radical and nonradical mechanisms. Normally, allyl radicals couple to give 1,5-hexadiene as the exclusive organic product;[36,37] in some instances, allyl radicals also decompose to give small amounts (<5%) of propene and allene.[38] Although the formation of 1,5-hexadiene as a byproduct in the CVD process is consistent with a radical mechanism, the formation of 2-methyl-1,4-pentadiene is not. Specifically, the formation of 2-methyl-1,4-pentadiene would have to involve isomerization of the allyl radical (CH_2=CH−CH_2•) to the isopropenyl radical (CH_2=C•−CH_3) by a 1,2-hydrogen shift, followed by coupling of the latter with an allyl radical; however, such a 1,2-hydrogen shift should be thermodynamically unfavorable due to the loss of resonance energy and the lower stability of alkenyl radicals.[39]

The thermal stabilities and decomposition chemistry of $Zn(allyl)_2$ and $Zn(2-methylallyl)_2$ in deuterated solvents have been studied by ^1H NMR spectroscopy.[40] In both cases, the sole organic species generated upon thermolysis at 100−150 °C were the allyl coupling products 1,5-hexadiene and 2,5-dimethyl-1,5-hexadiene, respectively; the authors concluded that these molecules decompose in solution via radical pathways. The formation of nontrivial amounts of propene and 2-methyl-1,4-pentadiene under CVD conditions however suggests that the decomposition pathways occurring on surfaces are not the same as those in solution.

It is our contention that all of the products generated during deposition of zinc from **1** and **2** can be accounted for without invoking the intermediacy of free radicals. On a clean metal surface, some of the allyl groups of the bis(allyl)zinc precursors decompose to give adsorbed hydrogen atoms and hydrocarbon fragments: the former react with intact allyl groups to give propene while the latter eventually give rise to 2-methyl-1,4-pentadiene and a carbonaceous overlayer. After the carbonaceous overlayer has been formed, however, the fragmentation of allyl groups is inhibited and allyl−allyl coupling reactions dominate during the rest of the deposition process.

The UHV studies show that 2-methyl-1,4-pentadiene and propene are formed under the same conditions: i.e., when the surface is relatively free of a carbonaceous overlayer and some of the allyl groups are being dehydrogenated to create a reservoir of surface-bound hydrogen atoms. One pathway seems most likely to account for the formation of 2-methyl-1,4-pentadiene during the deposition of zinc from **1**. The allyl dehydrogenation process could involve transfer of the 2-hydrogen atom of an allyl group to the surface to generate a surface-bound allene (CH_2=C=CH_2) molecule; subsequent attack of an intact allyl group at the electrophilic central carbon atom of allene, followed by reattachment of a hydrogen atom gives 2-methyl-2,4-pentadiene (Scheme 1).[41] This pathway also explains why substituted pentadienes are not generated during the deposition of zinc from bis(2-methylallyl)zinc, since there is no hydrogen at the 2 position and an allene intermediate cannot be generated.

However, loss of the 2-hydrogen atom of the allyl group is probably not the only dehydrogenation pathway; most likely, the fragmentation of the allyl groups can occur in a variety of ways to generate the reservoir of hydrogen atoms needed for the hydrogenation of surface-bound allyl groups to propene. Specifically, the dehydrogenation of 2-methylallyl groups on clean Pt surfaces must involve the terminal hydrogen atoms or the methyl group (or both). In summary, the mechanism by which zinc is deposited from bis(2-methylallyl)-zinc is evidently very similar to the mechanism by which

(36) Klein, R.; Kelley, R. D. *J. Phys. Chem.* **1975**, *79*, 1780−1784.
(37) Rossi, M.; King, K. D. Golden, D. M. *J. Am. Chem. Soc.* **1979**, *101*, 1223−1230.
(38) Al-Sader, B. H.; Crawford, R. J. *Can. J. Chem.* **1970**, *48*, 2745−2754.
(39) March, J. *Advanced Organic Chemistry*, 4th ed.; Wiley, New York, 1992; pp 191−193.
(40) Benn, R.; Hoffmann, E. G.; Lehmkuhl, H.; Nehl, H. *J. Organomet. Chem.* **1978**, *146*, 103−112.
(41) An alternative mechanism, attack of one surface-bound allyl group on the central carbon of another followed by a 1,2-hydrogen shift, is less likely since this process would not account for the observation that the generation of propene and 2-methyl-2,4-pentadiene is correlated.

Scheme 1. Proposed Surface Reactions of Allyl Groups Showing the Formation of 1,5-Hexadiene, Propene, 2-Methyl-1,4-pentadiene, and the Carbonaceous Overlayer

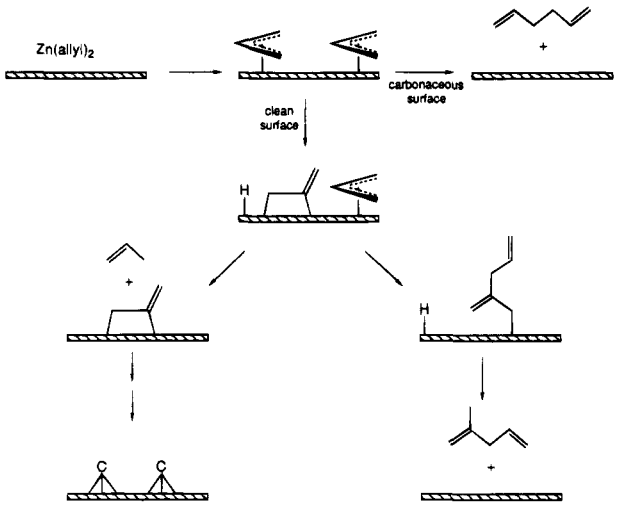

zinc is deposited from bis(allyl)zinc, except that the latter molecule can more easily generate allene intermediates.

Finally, although we cannot categorically rule out the possibility that gas-phase reactions are important during the deposition of zinc from these zinc allyl precursors under CVD conditions, the similarity of the product distributions to those seen under UHV conditions (where gas-phase chemistry is certainly unimportant) suggests that all of the reactions are indeed surface-promoted.

Deposition of Multicomponent Films. One of the interesting aspects of the MOCVD process is that it can be used to deposit multicomponent films and heterostructures. We became interested in determining whether alloy and multilayer phases could be deposited from diallyl zinc in combination with other MOCVD precursors. Accordingly, the CVD of mixtures of zinc and palladium was investigated using allylzinc and allylpalladium[20,21] complexes as precursors.

For these studies, a CVD apparatus equipped with two sample dosing lines was employed because the precursors have different vapor pressures (the Pd complex is more volatile). Simultaneous passage of bis(2-methylallyl)palladium and bis(2-methylallyl)zinc (in an approximate 5:1 ratio) over a Si wafer at 250 °C and 10^{-2} Torr results in the deposition of a film containing Pd and Zn. The Pd to Zn ratio in the deposit (5:1) is similar to that of the precursor mixture as judged from the AES depth profile (Figure 10).[42] The X-ray diffraction profile shows a strong peak at a *d* spacing of 2.148 Å and weaker features at 2.723, 2.341, and 1.418 Å; these do not correspond to the peaks expected from either pure palladium or pure zinc (Figure 11) and imply that a Pd/Zn intermetallic compound had formed. When a 1:1 ratio of the precursors is passed over a copper foil,

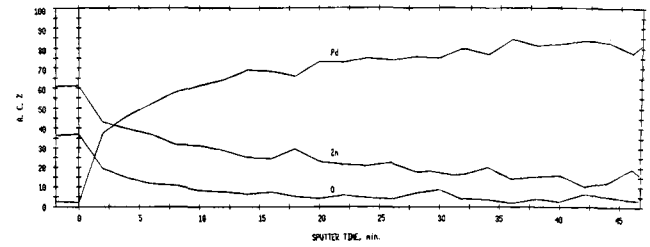

Figure 10. AES depth profile of a Pd/Zn alloy deposited from Pd(2-methylallyl)$_2$ and Zn(2-methylallyl)$_2$ on Si(100) at 250 °C and 10^{-2} Torr.

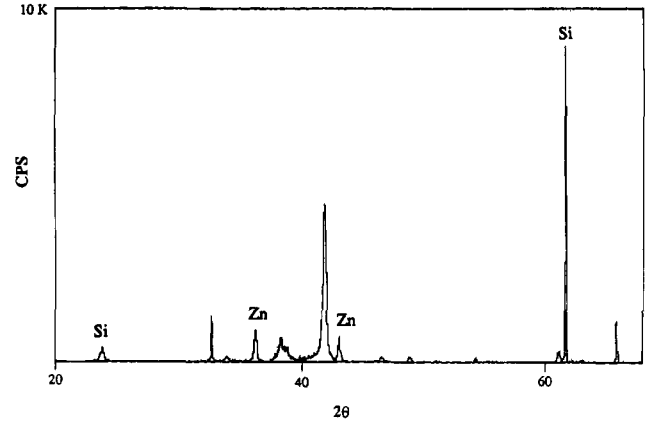

Figure 11. X-ray powder diffraction profile of a Pd/Zn alloy deposited from Pd(2-methylallyl)$_2$ and Zn(2-methylallyl)$_2$ on Si(100) at 250 °C and 10^{-2} Torr.

a deposit with approximately equal amounts of Zn and Pd is obtained. XRD suggests that this deposit is an amorphous alloy.

Palladium and zinc form a solid solution over a broad range of compositions.[43] Diffraction patterns for alloys of composition PdZn, $Pd_{3.9}Zn_{6.1}$, and $PdZn_2$ are known, and the strongest peaks were found at *d* spacings of 2.19, 2.15, and 2.22 Å, respectively.[44] Our results suggest that Zn/Pd alloys can also be deposited from organometallic CVD precursors.

Concluding Remarks

We have shown that bis(allyl)zinc compounds can serve as precursors for the deposition of zinc at temperatures as low as 150 °C. Even though the bis(allyl)zinc compounds are solids and have lower vapor pressures than dimethyl- and diethylzinc, these new precursors offer several advantages. Most importantly, they decompose at temperatures some 100 °C lower, and this can be a very useful advantage in the preparation of II-VI and doped III-V semiconductors, where high temperatures must be avoided to prevent the formation of crystal defects. The bis(allyl)zinc precursors afford clean zinc deposits at reasonable rates even in the absence of hydrogen as a carrier gas. If liquid allylzinc compounds can be developed, they could be very attractive candidates to replace alkylzinc compounds as precursors for zinc deposition.

Spectroscopic studies under ultra high vacuum conditions show that bis(allyl)zinc reacts differently depend-

(42) Although the X-ray diffraction pattern suggests that some metallic zinc may be present in the uppermost layers of the deposit, the Auger depth profiles clearly show that in the interiors of the films (after ca. 15 min sputtering), the Pd to Zn ratio is ca. 5:1. The depth profiles also suggest that the zinc concentration decreases slightly and the palladium concentration increases slightly with increasing depth; however, this effect may be a consequence of the preferential sputtering of zinc under argon ion bombardment.

(43) Hansen, M. *Constitution of Binary Alloys*, McGraw-Hill: New York, 1958; pp 1130-1133.

(44) *JCPDS Powder Diffraction File*; McClune, W. F., Ed.; International Center for Diffraction Data: Swarthmore, PA, 1990.

ing on the nature of the surface: on clean surfaces some of the allyl groups fragment to provide a population of surface hydrogen atoms which couple with other allyl groups to form propene. In contrast, on surfaces that have a carbonaceous overlayer, the allyl groups reductively eliminate as 1,5-hexadiene. Under actual CVD conditions, only the initial stages of zinc deposition involve fragmentation of the allyl groups; most of the deposition chemistry (i.e., the steady-sate reactions responsible for zinc deposition) takes place in the presence of a carbonaceous overlayer. This carbonaceous material does not become trapped in the film interiors but instead remains at the surface of the growing zinc deposit.

Experimental Section

General Methods. All manipulations were carried out using standard Schlenk and cannula techniques under argon or in vacuum. Pentane, diethyl ether, and benzene were distilled from sodium–benzophenone ketyl under N_2 before use. $ZnCl_2$ (Aldrich) was dried with thionyl chloride at reflux. Allyl chloride (Aldrich) and 2-methylallyl chloride (Aldrich) were washed successively with 12 M HCl, saturated aqueous Na_2CO_3, and water, dried with $CaCl_2$ over night, and distilled before use. Magnesium turnings (Aldrich) were used as received. The allyl Grignard reagents $(C_3H_5)MgCl$ and $(2\text{-}MeC_3H_4)MgCl$ were prepared by a literature route.[45]

Elemental analyses were performed by the School of Chemical Sciences Microanalytical Laboratory at the University of Illinois. ^1H and ^{13}C NMR spectra were recorded on a General Electric QE 300 instrument at 300 and 75.44 MHz, respectively. ^1H and ^{13}C NMR chemical shifts are reported in δ units relative to $SiMe_4$ (positive chemical shifts to higher frequency). A Hewlett-Packard 5890 gas chromatograph equipped with a 30 m RSL-160 (5 μm thick poly(dimethylsiloxane) film, 0.32 mm i.d., Alltech) column and a 5970 series mass selective detector was used to obtain the GC/MS data. The mass selective detector was calibrated by using the 31, 50, and 69 amu peaks of perfluorotributylamine.

X-ray photoelectron spectra were recorded on a Perkin Elmer PHI-5400 ESCA system with a 15 kV, 400 W Mg Kα radiation source (1253.6 eV) under an operating pressure of ca. 10^{-10} Torr. The spectrometer was calibrated with the Au $f_{7/2}$ peak at 83.8 eV. Spectra were taken with a pass energy of 89.45 eV for the survey analyses and 17.9 eV for the multiplex analyses with an energy resolution of 0.5 eV. Auger electron spectra were recorded on a Perkin-Elmer PHI-660 AES system with a beam energy of 3 kV and a beam current density of ca. 5 $\mu A/cm^2$ under an operating pressure of ca. 10^{-10} Torr. XPS and AES spectra were collected after the samples had been argon-sputtered to remove surface contaminants. X-ray powder diffraction data were recorded on a Rigaku D-Max instrument using Cu Kα radiation with a power supply of 40 kV and 20 mA. Scanning electron micrographs were obtained on a ISI DS-130 instrument. Electrical conductivities were measured by painting silver electrodes (GC Electronics Silver Print conductive paint) on the surface of the film and measuring the resistance (Hewlett-Packard 3465B digital multimeter). Film thicknesses were determined with a Dektak 3030 stylus profilometer.

Bis(allyl)zinc.[29] To C_3H_5MgCl (320 mL of a 0.45 M solution in Et_2O, 130 mmol) at 0 °C was added dropwise a suspension of $ZnCl_2$ (7.5 g, 55 mmol) in diethyl ether (50 mL) over 1.5 h. After the addition was complete, the reaction mixture was warmed to room temperature, stirred for 20 h, and allowed to stand for an additional 5 h. The yellow solution was filtered and the solvent was removed under vacuum at room temperature to give a yellow solid. The solid was sublimed at 50 °C and 10^{-3} Torr onto a water-cooled coldfinger to give bright yellow microcrystals. Yield: 2.7 g (35%). Anal. Calcd for $C_6H_{10}Zn$: C, 48.8; H, 6.85; Zn, 44.3. Found: C, 48.7; H, 6.98; Zn, 44.0.

Bis(2-methylallyl)zinc.[29] To $2\text{-}MeC_3H_4MgCl$ (300 mL of a 0.28M solution in Et_2O, 84 mmol) at 0 °C was added dropwise a suspension of $ZnCl_2$ (5.7 g, 42 mmol) in diethyl ether (30 mL) over 40 min. After the addition was complete, the reaction mixture was warmed to room temperature, stirred for 2 h, and allowed to stand for 1 h. The yellow solution was filtered and the solvent was removed under vacuum at room temperature to give a yellow solid. The solid was sublimed at 50 °C and 10^{-3} Torr onto a water-cooled coldfinger to give bright yellow microcrystals. Yield: 2.2 g (30%). Anal. Calcd for $C_8H_{14}Zn$: C, 54.7; H, 8.04; Zn, 37.2. Found: C, 53.7; H, 8.00; Zn, 37.6.

Metal–Organic Chemical Vapor Deposition of Zinc. Chemical vapor deposition of zinc onto Si(100) wafers, quartz, copper, and aluminum substrates was studied in two different low-pressure CVD systems. In one apparatus,[21] ca. 0.3 g of the precursor was introduced into a Pyrex vacuum system via a breakseal ampule after the system had been baked out at 200 °C and ca. 10^{-4} Torr for 24 h. Substrates up to 8 × 3 cm in size were mounted on a resistively heated stage whose temperature was monitored with a thermocouple. A quadrupole mass spectrometer, interfaced to the system just downstream of the hot zone, allow in situ analyses of the gaseous products generated during deposition. The precursor reservoir and glass tubing leading to the deposition zone were maintained at 50 °C to provide a satisfactory transport rate of the precursor to the hot zone. Over deposition times of about 4 h, deposits of up to 10 μm in thickness could be grown.

The other deposition apparatus[46] had a smaller hot zone than the one above; it also has a lower pumping speed and a vacuum limit of 10^{-2} Torr. The Pyrex hot zone was heated externally, and could accommodate substrates up to 7 × 2 cm in size; the substrates rested on a collar. The precursor reservoir, which was charged with ca 0.3 g of the allyl zinc compound in a dry box, was attached to the apparatus after the hot zone was baked out at 200 °C at 10^{-2} Torr for 10 h. Typically, the deposition time was about 3 h and deposits of 20 μm in thickness could be grown.

Static Vacuum CVD Studies and Analysis of Gaseous Byproducts. To collect and analyze quantitatively the gaseous products generated under CVD conditions, $Zn(C_3H_5)_2$ was thermolyzed under a static vacuum (10^{-2} Torr) at 290 °C in a closed-system CVD apparatus. This apparatus consisted of a solvent reservoir, a precursor reservoir, a deposition zone, and an NMR tube.[47] The solvent reservoir was charged with a degassed mixture of benzene and benzene-d_6. [The concentration of protons in this solvent (2.995×10^{-3} mol of proton/g solvent) was established by dissolving hexamethylbenzene (0.0142 g, 0.87 mmol) in the solvent mixture (0.570 g) and measuring the intensity of the C_6H_6 peak relative to the C_6Me_6 peak in the ^1H NMR spectrum taken with a 120 s postacquisition delay.] During the thermolysis step, the solvent reservoir was isolated from the rest of the apparatus.

The precursor reservoir was charged with $Zn(C_3H_5)_2$ (0.103 g, 0.70 mmol) and cooled to −78 °C. The apparatus was evacuated to 10^{-2} Torr, and the hot zone was heated externally to 280 °C; after bakeout, the apparatus was isolated from the pump and kept under a static vacuum. The NMR tube was cooled to −196 °C, and the precursor reservoir was heated at 50 °C to sublime the $Zn(C_3H_5)_2$ through the deposition zone. A bright silvery film deposited on the walls of the deposition zone, and the organic byproducts were collected in the NMR tube. After the precursor had sublimed and the deposition was complete, the deposition zone was cooled to room temperature. The benzene/benzene-d_6 solvent mixture (0.396 g) was then transferred into the NMR tube, which was flame sealed. The tube contents were analyzed by ^1H and ^{13}C NMR spectroscopy. Integration errors due to differences in the

(45) O'Brien, S. *J. Chem. Soc. A* **1970**, 9–13.

(46) Jensen, J. A. Ph.D. Thesis, University of Illinois at Urbana–Champaign, May 1988.

(47) This apparatus has been described elsewhere; see: Jeffries, P. M.; Dubois, L. H.; Girolami, G. S. *Chem. Mater.* **1992**, *4*, 1169–1175.

spin–lattice relaxation times were minimized by using post-acquisition delay times greater than 5 times the longest T_1 and, for ^{13}C NMR spectra, NOE effects were suppressed by turning the decoupler off between acquisitions.

The ^1H and $^{13}C\{^1H\}$ NMR spectra of the organic products from the static vacuum CVD experiment showed the presence of 1,5-hexadiene along with small amounts of 2-methyl-1,4-pentadiene and propene. From the relative intensities of the C_6H_6, CH_2=$CHCH_2CH_2CH$=CH_2, CH_2=$CMeCH_2CH$=CH_2, and CH_2=$CHMe$ peaks in the $^{13}C\{^1H\}$ NMR spectrum (17.02, 14.18, 1.33, and 1.0), it was established that 4.945×10^{-4} mol of 1,5-hexadiene, 9.56×10^{-5} mol of 2-methyl-1,4-pentadiene, and 7.02×10^{-5} mol of propene had been generated. After NMR analysis of the byproducts, the sealed NMR tube was broken and the volatile organic byproducts were analyzed by GC/MS. The presence of the byproducts detected by NMR spectroscopy was confirmed.

The reflective silvery film that deposited in the hot zone was collected and analyzed. Microanalyses of the bulk films show the deposits to be nearly pure zinc: Found: Zn, 98.2; C, <0.3; H, <0.3.

The static vacuum CVD thermolysis of $Zn(Me-C_3H_4)_2$ was carried out using the same procedure as above. Amounts of reagents used: $Zn(Me-C_3H_4)_2$ (0.108 g, 0.62 mmol), benzene/benzene-d_6 (0.473 g). The relative intensities of the C_6H_6, CH_2=$CMeCH_2CH_2CMe$=CH_2, Me_2C=$CHCH$=CMe_2, and Me_2C=CH_2 peaks in the ^1H NMR spectrum (16:22.75:1:1) showed that 5.04×10^{-4} mol of 2,5-dimethyl-1,5-hexadiene, 4.43×10^{-5} mol of 2,5-dimethyl-2,4-hexadiene, and 4.43×10^{-5} mol of isobutylene were present.

The bright silvery deposit was shown to be zinc by microanalysis: Found: Zn, 99.6; C, <0.2; H, <0.2.

Ultrahigh Vacuum Studies. TPD and AES experiments were performed in a diffusion and titanium-sublimation-pumped ultrahigh-vacuum chamber with a base pressure of ca. 1×10^{-10} Torr. The system was equipped with four-grid low-energy electron diffraction optics (Varian), a single-pass cylindrical mirror analyzer (PHI) for Auger electron spectroscopy, and a differentially pumped quadrupole mass spectrometer (Vacuum Generators) for temperature-programmed desorption. During the TPD and integrated desorption mass spectrometry experiments, the heating rate was 1 K/s.

RAIR experiments were performed in a second, turbomolecular-pumped UHV system. Spectra were collected in reflection mode using a Fourier transform infrared spectrometer (Mattson Instruments) and a liquid nitrogen cooled, narrow band, MCT detector. Typically, 2048 scans were averaged at 4 cm^{-1} resolution. In the variable temperature experiments, the temperature of the crystal was raised to the indicated temperature for ~2 s and then cooled to the dosing temperature before data collection was initiated.

A 1 cm diameter Cu(111) single-crystal disk (>99.999%, Monocrystals) was oriented, cut, and polished using standard techniques. The sample was mounted on a molybdenum heater stage which could be heated to 1200 K via a tungsten filament or cooled to 100 K via copper braids connected to a liquid nitrogen reservoir. A chromel–alumel thermocouple, mounted on the side of the crystal, was used to monitor the sample temperature. The copper single crystal was cleaned by cycles of sputtering with Ne^+ (1 keV, 20 $\mu A/cm^2$) at both 300 and 900 K followed by annealing at 900 K. The crystal was sputtered and annealed before each experiment and its cleanliness was monitored by AES.

Dosing with bis(allyl)zinc was carried out with an effusive molecular beam doser. The mass spectrometer skimmer was held about 1 mm from the surface of the crystal during TPD and IDMS experiments.

Acknowledgment. We thank the Department of Energy under Grant DEFG02-91ER45439 for support of this work. Auger, XPS, XRD, and SEM studies were carried out in the Center for Microanalysis of Materials at the University of Illinois, which is supported by the Department of Energy under the same contract.